Dynamic control of magnetically trapped indirect excitons using external magnetic bias: Transition from two- to one-dimensional lattice

A. Abdelrahman and Byoung S. Ham

Center for Photon Information Processing, School of Electrical Engineering, Inha University, Incheon 402-751, South Korea

(Received 9 October 2012; revised manuscript received 1 January 2013; published 26 March 2013)

We demonstrate an on-demand spatial control of excitonic magnetic lattices for the potential applications of excitonic-based quantum optical devices. A two-dimensional magnetic lattice of indirect excitons can form a transition to a one-dimensional lattice configuration under the influence of external magnetic bias fields. The transition is identified by measuring the spatial distribution of two-dimensional photoluminescence for several values of the external magnetic bias fields. The number of trapped excitons is found to increase between sites along a perpendicular direction exhibiting a two- to one-dimensional lattice transition. This work may apply for various controllable quantum simulations, such as superfluid-Mott-insulators, in quantum optical devices.

DOI: 10.1103/PhysRevB.87.125311 PACS number(s): 73.21.Fg, 71.35.Ji, 52.55.Jd, 52.55.Lf

I. INTRODUCTION

Trapping of excitonic quasiparticles in a solid-state medium using electric or magnetic fields has recently become an active field of interest in the area of semiconductor physics. The two trapping mechanisms are rapidly gaining credit for their promise to underlie basic concepts of condensed matter systems. For example, it is now possible to create one- and two-dimensional latticelike configurations of electrically trapped indirect excitons (a bound state of electron holes) in a system of coupled quantum wells (CQWs)[1–3] as well as using in-plane potential.[4–7] Electrostatic traps were observed in cold excitonic gases, whose advantages are extending the lifetime of the trapped excitonic particles as well as allowing us to observe the direct emission of their spontaneous coherence of the trapped indirect excitons.[8] In such an approach, the gate voltage controls the excitons energy, where the applied electric field perpendicular to the growth direction of the CQWs shifts the energy of the created indirect excitons. Moreover, the spatial distribution of the electric fields can configure a profile of a confining potential for the excitonic particles.[4,9,10] Accordingly, the electrical variable trapping field and its configurability made it possible to create *in situ* gate control for manipulating the trapped excitonic particles on a time scale that is shorter than their lifetimes.[5–7] On the other hand, magnetic field confinement has emerged recently as an alternative stable trapping mechanism that can be used to confine excitonic particles in solid mediums.[11–15] After its successful implementation in an atomic medium, magnetic traps have shown extremely stable trapping and a long coherence lifetime of the trapped particles.[16] These magnetic traps can also be configured to shape one- and two-dimensional magnetic lattices of the trapped particles.[15–17] The impeded magnetic trapping fields in semiconductors can be realized by integrating a fabricated permanent magnetic material, such as a form of magnetic thin film, with a system of CQWs.[14,15] The magnetic thin film can then be patterned according to a desirable spatial distribution of the magnetic trapping potentials. Similar to electrical traps, the shape and depth of the magnetic traps can be controlled by using external magnetic bias fields. In this approach, excitonic particles are created in CQWs and trapped by magnetic fields representing two-dimensional magnetic lattices of indirect excitons. This approach can be adopted to simulate condensed matter systems where strongly correlated systems such as the transition of a superfluid-Mott-insulator (SF-MI) can be achieved.[18] In this article, we demonstrate a dimensional active control of the magnetic lattice configuration of indirect excitons by applying external magnetic bias fields.

II. TWO-DIMENSIONAL MAGNETIC LATTICES

To create a magnetic lattice of indirect excitons, periodically distributed magnetic field local minima $B_{\min}$ and maxima $B_{\max}$ are projected onto the indirect-exciton formation plane of the CQWs.[15] The inhomogeneous magnetic fields that used to trap the excitonic particles are originated from a specific pattern permanently magnetized thin film.[17] Figure 1(a) shows an example of two-dimensional arrays of the permanent magnetic square holes. The projected magnetic field local minima and maxima introduce periodic confining space (single traps) onto the plane of the CQWs, where the confinement mechanism acts the role of magnetic trapping of ultracold atoms.[16,17,19]

An analytical model to describe the confining magnetic fields at a working distance $z_{\min}$ from the surface of the thin film can be written as follows:[17]

$$\begin{aligned} B(x,y,z) = \{ & B_{x\,\mathrm{bias}}^2 + B_{y\,\mathrm{bias}}^2 + B_{z\,\mathrm{bias}}^2 + 2B_0^2 e^{-2\beta(z-\tau)} \\ & \times [1+\cos(\beta x)\cos(\beta y)] + 2B_0^2 e^{-\beta(z-\tau)} \\ & \times (B_{x\,\mathrm{bias}}\sin(\beta x) + B_{y\,\mathrm{bias}}\sin(\beta y) \\ & + [\cos(\beta x)+\cos(\beta y)]B_{z\,\mathrm{bias}}) \}^{1/2}. \end{aligned} \tag{1}$$

External magnetic bias fields are denoted by $B_{x,y,z\,\mathrm{bias}}$, and the thickness of the permanently magnetized thin film is characterized by the parameter τ, which is set to be equal to 2 μm in both the simulation and the experiment. The B_0 is the reference magnetic field defined by $B_0 = \tilde{B}(1-e^{-\beta\tau})$ with $\beta = \pi/\alpha$, where α represents both the length α_h of each fabricated pattern and their separating distances α_s, as shown in Fig. 1(a). The $\tilde{B}$ is magnetic induction, $\tilde{B} = \frac{\mu_0 M_z}{\pi}$, where M_z is the magnetization of the thin film. The distribution of the magnetic lattice sites (single traps) is periodic according to Eq. (1), and the positions of the local field minima $B_{\min}$

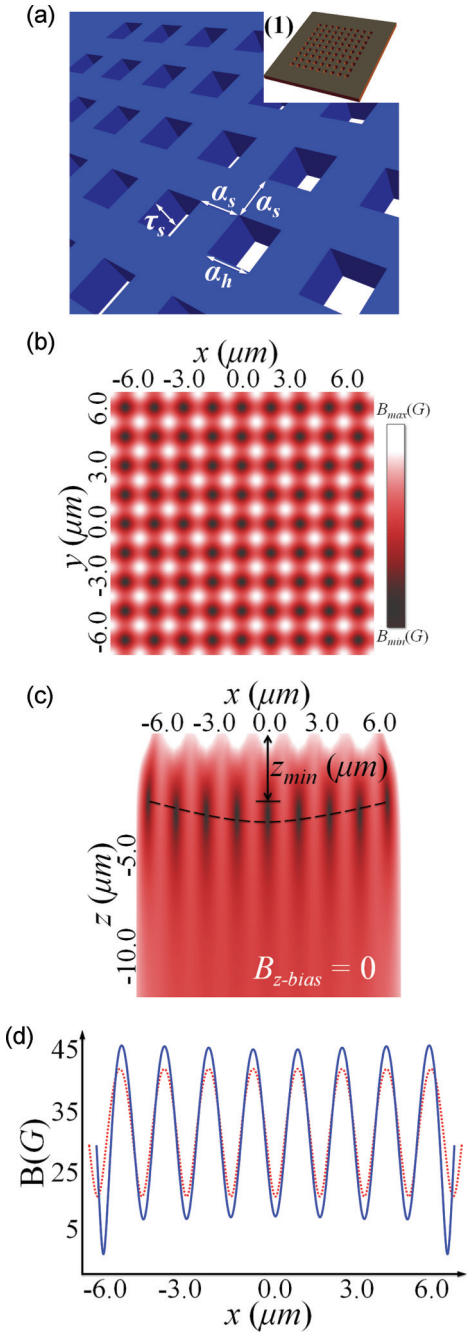

FIG. 1. (Color online) (a) Simulation model of a permanent magnetic material thin film with a thickness of $\tau = 2\ \mu$m used to generate the two-dimensional magnetic lattice [inset (1) shows a block of 9×9 square holes]. The lattice is created with a periodicity of $\alpha_s = \alpha_h = \alpha = 2\ \mu$m. (b) Density plot of the simulated lattice shows the distributed single traps across the x/y plane at the local minima using an analytical expression [Eq. (1)], and (c) numerically calculated trapping fields across the x/z plane, where the dashed line indicates the asymmetrical distribution of the sites along the z axis. (d) Numerical (solid line) and analytical (dashed line) calculations of the inhomogeneous magnetic field at a trapping level [i.e., $z = z_{\min}\ (\mu$m)].

are $x_{\min} = n_x\alpha, n_x = 0, \pm 1, \pm 2, \ldots, y_{\min} = n_y\alpha, n_y = 0, \pm 1, \pm 2, \ldots$, and $z_{\min} = \frac{\alpha}{\pi}\ln(B_0)$.

Figure 1(a) shows the model used to simulate the magnetic lattice, and Fig. 1(b) shows a magnetic lattice created at the plane of CQWs simulated by the analytical expression in Eq. (1). In the experimental setup, each fabricated single pattern takes the shape of a square hole, where a set of $n \times n$ square holes is regarded as one block as shown in the inset of Fig. 1(a). The 3×3 blocks are fabricated, where each block consists of 9×9 square holes. As explained in the experimental details, the coupled quantum wells are allocated at $z = z_{\min}\ (\mu$m). However, due to the asymmetrical effect (that is, the inhomogeneous spatial distribution of the lattice sites) across the $x, y/z$ plane, each confining area at the CQW plane (i.e., at each individual lattice site) experiences a different minimum value of trapping potential: This effect is indicated by the dashed line in Fig. 1(c). In other words, at zero-bias fields, the center sites have smaller values of the magnetic local minima $B_{\min}$ (G) in comparison with the edge sites whose values are higher when measured at the confining plane of the coupled quantum wells [i.e., $B_{\min}^{\text{center}} < B_{\min}^{\text{edge}}$ (G)]. The asymmetrical distribution of the sites creates periodically distributed potential tilts across the x/y plane which initially existed after magnetization.[17] The potential tilt is essential to allow the tunneling of trapped particles between the lattice sites, where the tunneling is the key mechanism of the present active control of the excitonic lattice transition.

The gradient (or the curvature) of the magnetic field at the trapping position is of a particular interest, where a trapping field with a steeper gradient and zero local minima (or very close to zero) often develops the so-called Majorana spin-flip in magnetic traps.[20] However, this destructive process has not yet been observed in such magnetic lattices of indirect excitons. It is important at this stage to emphasize that the zero local minima can easily be avoided in the case of magnetic trapping in semiconductors via fabrication; the nonzero local minima can precisely be allocated at the confining plane of the quantum wells.

The trapping frequencies $\omega_{x,y}$ along the x and y confining directions (that is, across the x/y plane of confinement) depend strongly on the gradient of the inhomogeneous magnetic fields at each site, where in our calculations we determine the curvatures of the trapping field along the x/y axis as follows:

$$\frac{\partial^2 B}{\partial x^2} = -\beta^2 B_0 e^{\beta(z-\tau)}\left\{\frac{\cos(\beta x)\cos(\beta y)}{\sqrt{2+2\cos(\beta x)\cos(\beta y)}} + \frac{\cos^2(\beta x)\sin^2(\beta y)}{\sqrt[3]{2+2\cos(\beta x)\cos(\beta y)}}\right\}, \tag{2}$$

$$\frac{\partial^2 B}{\partial y^2} = -\beta^2 B_0 e^{\beta(z-\tau)}\left\{\frac{\cos(\beta x)\cos(\beta y)}{\sqrt{2+2\cos(\beta x)\cos(\beta y)}} + \frac{\cos^2(\beta y)\sin^2(\beta x)}{\sqrt[3]{2+2\cos(\beta y)\cos(\beta x)}}\right\}. \tag{3}$$

The trapping frequencies along the x and y axes are defined as

$$\omega_{\mathbf{r}} = \frac{\beta}{2\pi}\sqrt{\mu_B g_F m_F \frac{\partial^2 B}{\partial \mathbf{r}^2}} \quad \text{with} \quad \mathbf{r} \in \{x, y\}. \tag{4}$$

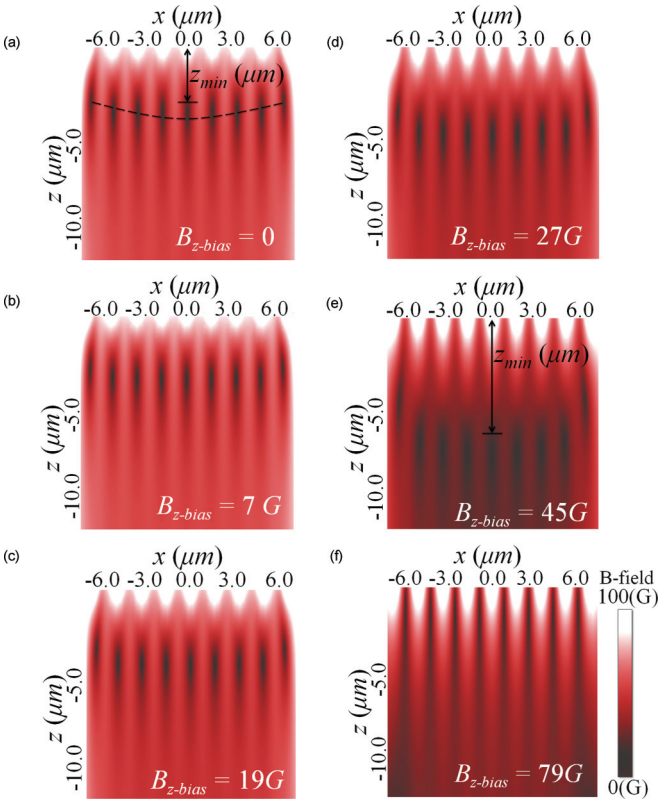

FIG. 2. (Color online) Numerical simulations for the effect of external magnetic bias field along the z axis. (a) The magnetic lattice is initially set at zero bias: $B_{z\,\mathrm{bias}} = B_{x\,\mathrm{bias}} = B_{y\,\mathrm{bias}} = 0$, $\alpha_s = \alpha_h = 2\ \mu\mathrm{m}$, $M_z = 2.8\,\mathrm{kG}$, $\tau = 2\ \mu\mathrm{m}$, $n = 9$ with local minima at $z_{\min} = 4\ \mu\mathrm{m}$. (b)–(e) Increasing the z-bias field ($B_{x\,\mathrm{bias}} = B_{y\,\mathrm{bias}} = 0, B_{z\,\mathrm{bias}} \neq 0$) causes the magnetic local minima to depart away from the thin-film surface deeper into and beyond the coupled quantum-well plane. (f) A collapse of the local minima occurs at high values of $B_{z\,\mathrm{bias}}$ at which the magnetic lattice is reshaped as shown in Fig. 3(f).

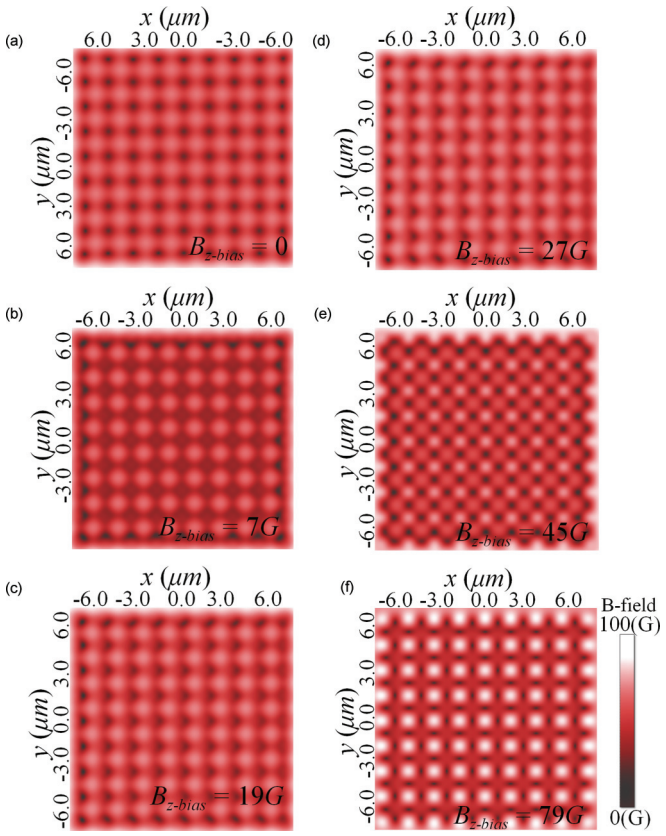

FIG. 3. (Color online) Numerical calculations for magnetic-field local minima distributed across the x/y plane at $z_{\min}$ with (a) no external magnetic bias field ($B_{z\,\mathrm{bias}} = B_{x\,\mathrm{bias}} = B_{y\,\mathrm{bias}} = 0$) for a lattice with the same initial parameter as in Figs. 2(b)–2(f). The shift of the lattice site locations and the deformation in their confining spaces with respect to the external z-bias field are as follows: $B_{x\,\mathrm{bias}} = B_{y\,\mathrm{bias}} = 0, B_{z\,\mathrm{bias}} \neq 0$. All x/y planes are simulated at the local minima along the z axis: $z_{\min} \approx 4\ \mu\mathrm{m}$.

The trapping frequency along the z axis is defined by $\omega_z = \omega_x + \omega_y$. In Eq. (4), m_F, μ_B, and g_F represent a magnetic quantum number, the Bohr magneton, and the Landé g factor, respectively. Each localized minimum is surrounded by magnetic barriers that define the space of the confinement and the depth of the traps, and the magnitude of the barrier is defined by $\Delta B(\mathbf{r}) = |B_{\max}(\mathbf{r})| - |B_{\min}(\mathbf{r})|$, while the depth of each trap is defined by $\Gamma(\mathbf{r}) = \frac{(\mu_B g_F m_F)}{k_B}\Delta B(\mathbf{r})$, where K_B is the Boltzmann constant.

Figures 2–5 show the numerical simulation results of a two-dimensional magnetic lattice created with the following parameters: $\alpha_h = \alpha_s = 2\ \mu\mathrm{m}$, $\tau = 2\ \mu\mathrm{m}$, $M_z = 2.8$ KG, and $n = 9$ holes. The working distance is found to be located at $z_{\min} = (2\alpha \pm \delta z)\ \mu\mathrm{m}$, where the magnetic lattice is initially set at $B_{x\,\mathrm{bias}} = B_{y\,\mathrm{bias}} = B_{z\,\mathrm{bias}} = 0$ as shown in Fig. 2(a).

To induce the tunneling of the magnetically trapped particles or to displace the site locations across the x/y plane and/or along the z axis, the external magnetic bias fields are applied along the x/y axis and/or the z axis. The application of the bias fields, specifically the $B_{z\,\mathrm{bias}}$ field, results in reducing the tunneling barrier between the sites and hence increasing the tunneling rate of the trapped excitons. The numerical simulation results shown in Figs. 2 and 3 are for the effect of the applied external bias field along the z axis. The external magnetic z-bias field increases (or decreases) the distance $z_{\min}$ between the surface of the permanently magnetized thin film and the initial position of the local field minima $B_{\min}$, i.e., the actual location of the lattice site along the z axis. As shown in Fig. 2(e), $B_{\min/\max}$ can be allocated at different distances from the plane of the coupled quantum wells, in which case the magnetic field at the trapping point is increased (decreased) resulting in a reduced (increased) number of trapped excitons. The z-bias field also causes the confining space to deform and to redistribute the lattice sites. As shown in Figs. 3(b)–3(f), such an effect allows the transition between different interesting configurations of the magnetic lattice.

On the other hand, external magnetic bias fields along the x axis and/or the y axis are used to reshape the magnetic lattices from two-dimensional to one-dimensional configuration. As shown in Figs. 5(b)–5(f), an external magnetic bias field along the x axis can cause the lattice sites to evolve from a two-dimensional to a one-dimensional distribution. The numerical simulation in Fig. 6 compares the values of the

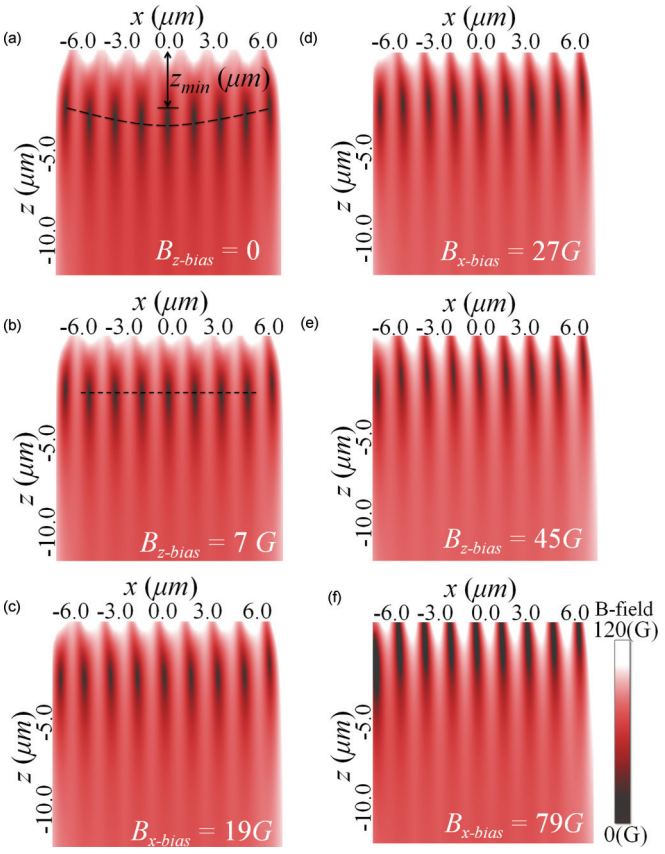

FIG. 4. (Color online) Using the same initial parameters of Fig. 2, a magnetic lattice subject to external magnetic bias field along the x axis $B_{x\,\mathrm{bias}}$ is simulated: $B_{x\,\mathrm{bias}} = B_{y\,\mathrm{bias}} = B_{z\,\mathrm{bias}} = 0$. (b)–(f) The effects of the applied external bias field along the x axis: $B_{y\,\mathrm{bias}} = B_{z\,\mathrm{bias}} = 0, B_{x\,\mathrm{bias}} \neq 0$. Oscillations between asymmetric [dashed line in (a)] and symmetric [dashed line in (b)] magnetic lattices can be controlled externally using the magnetic bias fields.

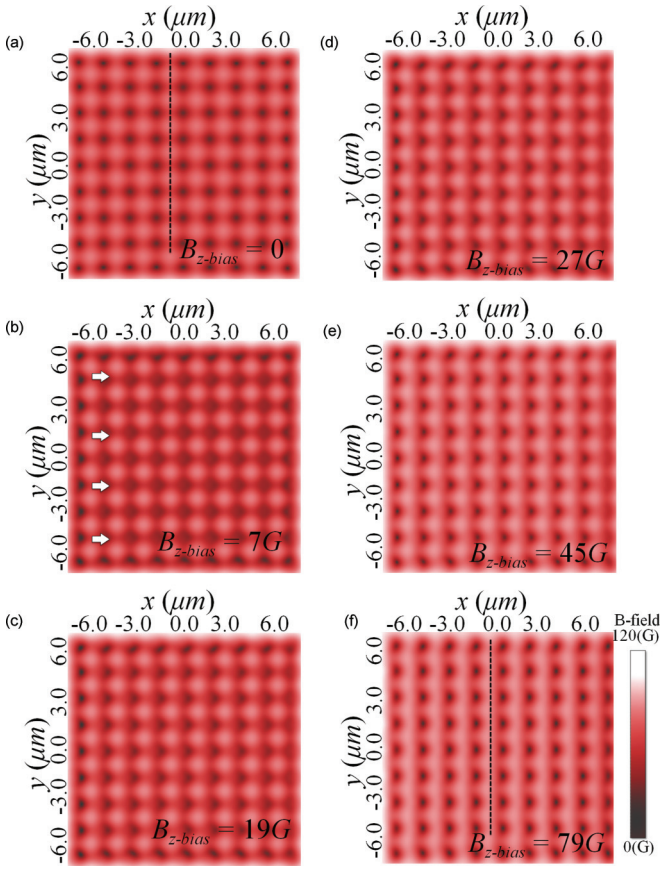

FIG. 5. (Color online) External magnetic x-bias field-induced lattice sites across the x/y plane. Sites in a two-dimensional magnetic lattice can align themselves in specific patterns according to the external bias fields such as the transition to a one-dimensional configuration (a)–(f). Initial parameters are the same as those in Fig. 2: $B_{x\,\mathrm{bias}} = B_{y\,\mathrm{bias}} = B_{z\,\mathrm{bias}} = 0$. (b)–(f) $B_{y\,\mathrm{bias}} = B_{z\,\mathrm{bias}} = 0, B_{x\,\mathrm{bias}} \neq 0$ at $z_{\mathrm{min}} \approx 4$ μm. Black arrows indicate the direction of the applied field.

magnetic fields at the tunneling barriers along the y axis of Figs. 5(a) and 5(f) (as indicated by the dotted lines). The B_{max} of the magnetic barriers between sites increase as $B_{x\,\mathrm{bias}} \neq 0$, which creates a one-dimensional lattice shape. Moreover, a combination of z axis and x/y axis external magnetic bias fields may enable a simulation of condensed-matter systems through reshaping the sites. For instance, it is possible to simulate the transition from/to Brillouin zones by redistributing the magnetically trapped excitonic particles across the lattice according to accurately adjusted external magnetic bias fields (this description also includes optically trapped atomic species[21]).

III. EXPERIMENTAL REALIZATION OF ON-DEMAND 2D TO 1D LATTICE TRANSITION IN AN EXCITONIC MAGNETIC LATTICE

In our recent experimental results,[15] we observed the formation of an excitonic two-dimensional magnetic lattice at a plane of coupled quantum wells. For the present experiments, the CQWs are grown by molecular-beam epitaxy, where there are two 8 nm GaAs quantum wells separated by a 4 nm $Al_{0.33}Ga_{0.67}As$ barrier. This CQW is deposited by a 200 nm $Al_{0.33}Ga_{0.67}As$ conducting layer on both sides. Metal contacts are deposited at the top and at the bottom of the sample to monitor the electric field along the z direction for generating indirect excitons. A nonmagnetic material gadolinium gallium garnet $Gd_3Ga_5O_{12}$ (GGG) of thickness $\simeq 3$ μm is deposited, using an rf-sputtering technique, on top of the CQW system. The thickness of the GGG nonmagnetic spacer is used to determine the effective distance z_{min} for allocating the magnetic field trapping local minima and maxima within the quantum-well layers. The permanent magnetic material ($Bi_2Dy_1Fe_4Ga_1O_{12}$) with a thickness of $\simeq 2$ μm is deposited on top of the sample of the (GGG + CQWs) using the rf-sputtering technique.

The integrated magnetic-CQWs sample is placed in an optical cryostat with a temperature fixed at 13 K, and the emitted PL images are collected using an objective microscope: For more details of the experimental methods, see Ref. 15. The indirect excitons are found to be self-trapped according to the two-dimensional distribution of the confining magnetic field, as shown in Fig. 7(a). As simulated in Fig. 5, an external magnetic bias field along the x axis is used to induce the bidirectional tunneling process between sites along the y axis,

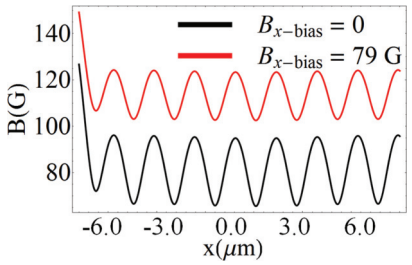

FIG. 6. (Color online) Comparing the values of the magnetic fields at the tunneling barriers along the y axis of Figs. 5(a) and 5(f) (indicated by the dotted lines). The $B_{\max}$ of the magnetic barriers between sites increase when $B_{x\,\text{bias}} \neq 0$ creating the one-dimensional lattice shape.

resulting in the observed 2D to 1D lattice transition as shown in Fig. 7. As shown in Fig. 7, the effect of gradually increasing the external magnetic bias field on the trapped indirect excitons is to reconfigure the shape of the magnetic lattice. Because the number of trapped particles per site changes according to the value of the externally applied magnetic field, the exciton redistribution in Fig. 7 strongly supports the theoretical calculations in Fig. 5.

Although the trapped excitonic gases are not sufficiently cooled, such 2D to 1D transition may lead to the realization of a possibly reversed cycle of self-trapped excitonic ultracold clouds to the intrasite superfluid state, to be reported elsewhere.[22–25] The reverse process can be achieved by decreasing the external magnetic bias fields, to be discussed elsewhere.

A scanning property of selected lattice sites along the y axis in Fig. 8(a) shows an increased number of trapped particles with the external magnetic x-bias field where such increments are because the values of the magnetic fields between sites

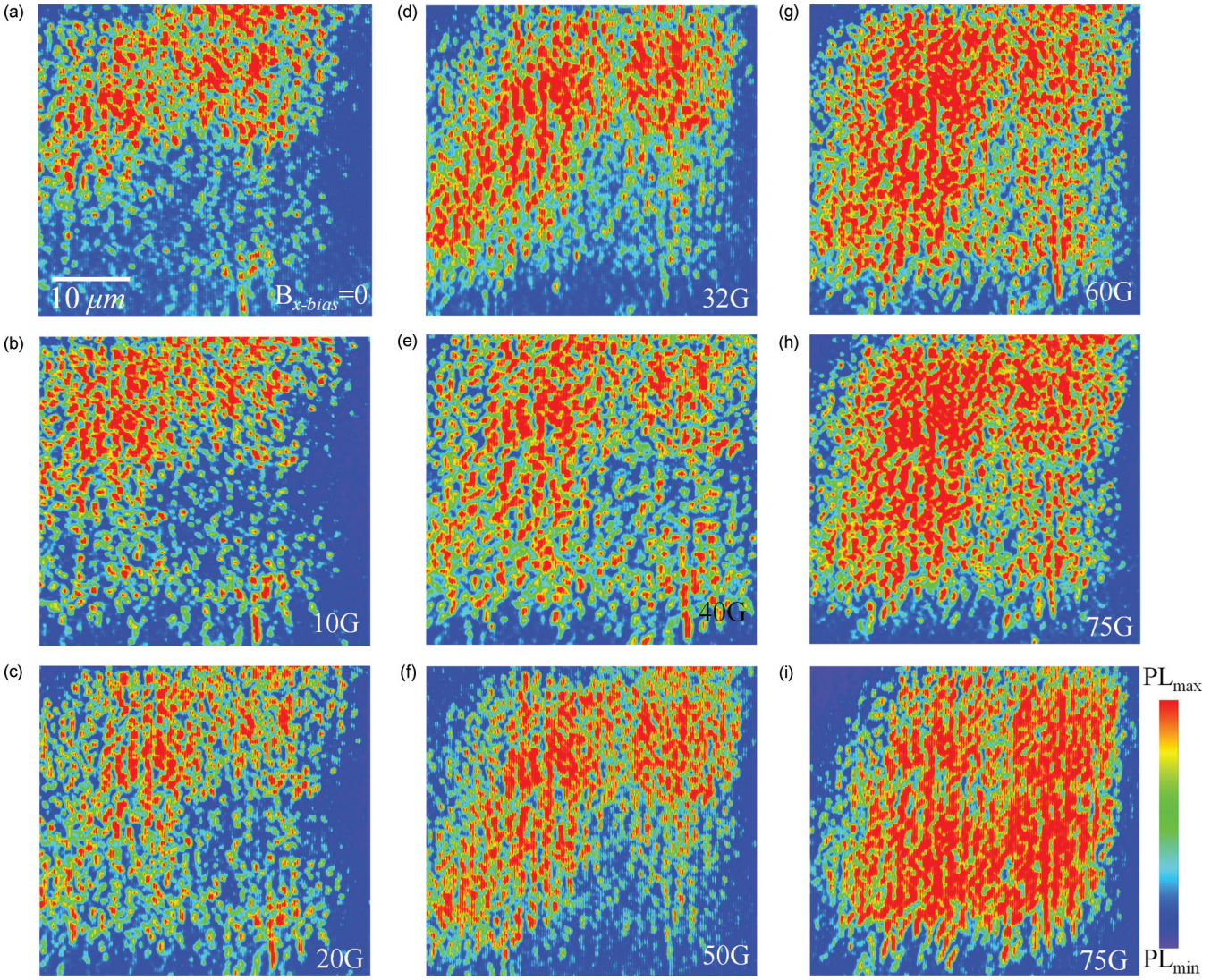

FIG. 7. (Color online) Experimental results of the magnetically trapped indirect excitons showing a 2D to 1D transition in a lattice configuration. The magnetic lattice is created with $\alpha_s = \alpha_h = 2$ μm, $M_z = 2.8$ kG, $\tau = 2$ μm, and $n = 9$. The local field minimum projected at the coupled quantum-well level is $z_{\min} \approx 2.5$ μm. An external magnetic bias field is applied along the x axis and gradually increases from 0 to 75 G, $B_{y\,\text{bias}} = B_{z\,\text{bias}} = 0, B_{x\,\text{bias}} = 0 \rightarrow 75$ G. (a)–(h) The gate voltage is 0.2 V. (i) The gate voltage increases to 0.3 V to emphasize the excitonic concentration in 1D space.

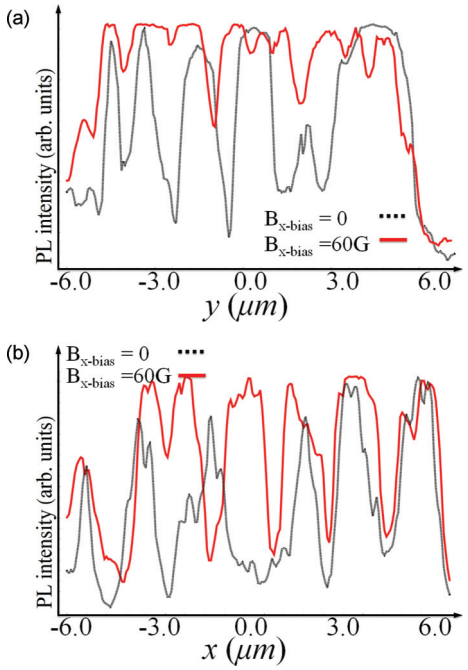

FIG. 8. (Color online) Measured PL intensity of the trapped indirect excitons across a selected number of lattice sites along the y axis, before and after the external magnetic bias field. External x-bias field increases the number of trapped particles between lattice sites (along the y axis) for 2D to 1D magnetic lattice transformation. (b) Measured PL intensity of the lattice sites along the x axis before and after the external x-bias field. The sites are also noticed to be displaced from their original positions with an increased number of trapped particles. Experimental conditions are the same as in Fig. 7.

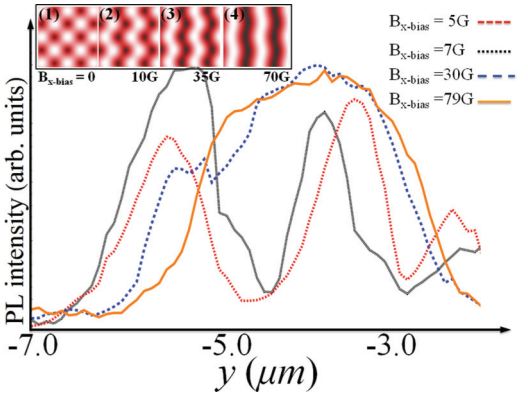

FIG. 9. (Color online) PL measurements of two adjacent lattice sites along the y axis for different external magnetic bias field applied in the x axis. According to analytical calculations of the magnetic field in the insets (1)–(4), more indirect excitons are trapped between the sites because of the decreased magnetic field values between sites along the y axis. Experimental conditions are the same as in Fig. 7.

along the y axis ($B_{y,\max}$) become close to or equal to the values of the actual individual traps, i.e., the $B_{y,\max} \simeq B_{\min}$. Figure 8(b) shows the shift of trap positions along the x axis with an increased number of trapped excitons where, as a result, the external bias field causes a slight shift of the sites along the applied field direction, i.e., the x direction. In Fig. 9, trapped excitons are compared for two adjacent sites along the y axis for different values of the external magnetic bias field applied along the x axis. The number of trapped particles between sites (in the valley along the y axis) increases as the value of the external bias field increases (along the x axis).

The results in Figs. 7–9 are in agreement with the simulation results of Fig. 5. A slight modification in the site position and the shape along the x axis of the lattice can be observed when applying external bias fields. The two- to one-dimensional lattice transition also occurs along the y axis at the field bias constraints as simulated.

Emphasizing the fact that the current approach is suitable to simulate condensed matter systems, one can consider the magnetic confining field to act as the potential confining fields between ions, and the magnetically trapped excitonic particles play the role of electrons. In such a model, the parameters are tunable without crystal-like disorders, in which case the sites of the magnetic lattice can be translated or rotated with a preserved dimensionality, i.e., the two-dimensional configuration. The magnetic confinement approach can be applied to accommodate a strongly correlated system such as the transition of a superfluid-Mott-insulator (MI) proposed by Jaksch *et al.*[18] and as was achieved in an atomic medium by Greiner *et al.*[26–28] Moreover, the preparation of the lattice in a MI state is a crucial step toward an efficient quantum register, where entanglement between the magnetically trapped excitons can be achieved by controlled collision using external magnetic bias fields.[29]

IV. CONCLUSION

A dimensional active control of a magnetic lattice of excitonic particles was demonstrated. Magnetically trapped indirect excitons in a two-dimensional lattice configuration can be controlled to transit into a one-dimensional magnetic lattice of excitons with applied external magnetic bias fields. The dimensional transition is identified by measuring the spatial distribution of the 2D PL intensity for several values of the external bias fields where the number of the trapped excitons increases in the valley between sites, at a certain direction, exhibiting a 1D lattice configuration. The trapped excitonic gases can be cooled sufficiently, in which case the observed transition may lead to a realization of the self-trapped excitonic ultracold clouds to intrasite superfluidity transition, to be reported elsewhere.

ACKNOWLEDGMENTS

This work was supported by the Creative Research Initiative Program (No. 2012-0000228) of the Korean Ministry of Education, Science and Technology via the National Research Foundation. B.S.H. acknowledges that this work was also supported by the Korea Communications Commission, S. Korea, under the R&D program supervised by the Korea Communications Agency (KCA-2012-12-911-04-003).

[1]M. Remeika, J. C. Graves, A. T. Hammack, A. D. Meyertholen, M. M. Fogler, L. V. Butov, M. Hanson, and A. C. Gossard, Phys. Rev. Lett. **102**, 186803 (2009).
[2]M. Remeika, M. Fogler, L. Butov, M. Hanson, and A. Gossard, Appl. Phys. Lett. **100**, 061103 (2012).
[3]Y. Kuznetsova, A. High, and L. Butov, Appl. Phys. Lett. **97**, 201106 (2010).
[4]S. Zimmermann, G. Schedelbeck, A. Govorov, A. Wixforth, J. Kotthaus, M. Bichler, W. Wegscheider, and G. Abstreiter, Appl. Phys. Lett. **73**, 154 (1998).
[5]J. Rudolph, R. Hey, and P. V. Santos, Phys. Rev. Lett. **99**, 047602 (2007).
[6]S. Lazi, P. Santos, and R. Hey, Physica E **42**, 2640 (2010).
[7]A. Winbow, J. Leonard, M. Remeika, Y. Kuznetsova, A. High, A. Hammack, L. Butov, J. Wilkes, A. Guenther, A. Ivanov *et al.*, Phys. Rev. Lett. **106**, 196806 (2011).
[8]A. High, J. Leonard, M. Remeika, L. Butov, M. Hanson, and A. Gossard, Nano Lett. **12**, 2605 (2012).
[9]M. Hagn, A. Zrenner, G. Böhm, and G. Weimann, Appl. Phys. Lett. **67**, 232 (1995).
[10]A. Gärtner, A. Holleitner, J. Kotthaus, and D. Schuh, Appl. Phys. Lett. **89**, 052108 (2006).
[11]J. A. K. Freire, A. Matulis, F. M. Peeters, V. N. Freire, and G. A. Farias, Phys. Rev. B **61**, 2895 (2000).
[12]J. A. K. Freire, F. M. Peeters, A. Matulis, V. N. Freire, and G. A. Farias, Phys. Rev. B **62**, 7316 (2000).
[13]Z. Koinov, G. Collins, and M. Mirassou, Phys. Status Solidi B **243**, 4046 (2006).
[14]A. Abdelrahman, H. Kang, S. Yim, M. Vasiliev, K. Alameh, and Y. Lee, J. Appl. Phys. **110**, 013710 (2010).
[15]A. Abdelrahman and B. S. Ham, Phys. Rev. B **86**, 085445 (2012).
[16]S. Whitlock, R. Gerritsmav, T. Fernholz, and R. Spreeuw, New J. Phys. **11**, 023021 (2009).
[17]A. Abdelrahman, M. Vasiliev, K. Alameh, and P. Hannaford, Phys. Rev. A **82**, 012320 (2010).
[18]D. Jaksch, C. Bruder, J. Cirac, C. Gardiner, and P. Zoller, Phys. Rev. Lett. **81**, 3108 (1998).
[19]M. Singh, R. McLean, A. Sidorov, and P. Hannaford, Phys. Rev. A **79**, 053407 (2009).
[20]D. M. Brink and C. V. Sukumar, Phys. Rev. A **74**, 035401 (2006).
[21]D. Clement, N. Fabbri, L. Fallani, C. Fort, and M. Inguscio, New J. Phys. **11**, 103030 (2009).
[22]S. Backhaus, S. Pereverzev, A. Loshak, J. Davis, and R. Packard, Science **278**, 1435 (1998).
[23]D. S. Hall, M. R. Matthews, C. E. Wieman, and E. A. Cornell, Phys. Rev. Lett. **81**, 1543 (1998).
[24]B. Anderson and M. Kasevich, Science **282**, 1686 (1998).
[25]A. Smerzi, S. Fantoni, S. Giovanazzi, and S. R. Shenoy, Phys. Rev. Lett. **79**, 4950 (1997).
[26]M. Greiner, O. Mandel, T. Esslinger, T. Hansch, and I. Bloch, Nature (London) **415**, 39 (2002).
[27]W. Bakr, A. Peng, M. Tai, R. Ma, J. Simon, J. Gillen, S. Folling, L. Pollet, and M. Greiner, Science **329**, 547 (2010).
[28]M. Greiner, O. Mandel, T. Hansch, and I. Bloch, Nature (London) **419**, 51 (2002).
[29]D. Jaksch, H. J. Briegel, J. I. Cirac, C. W. Gardiner, and P. Zoller, Phys. Rev. Lett. **82**, 1975 (1999).